Hybrid optical Tamm states in a planar dielectric microcavity

R. Brückner,* M. Sudzius, S. I. Hintschich, H. Fröb, V. G. Lyssenko, and K. Leo
Institut für Angewandte Photophysik, Technische Universität Dresden, D-01062 Dresden, Germany
(Received 7 October 2010; revised manuscript received 4 December 2010; published 31 January 2011)

Using spectroscopic experiments, we show the transition from a single cavity mode into two optical Tamm states upon incorporating a thin metal layer into a planar organic microcavity. The eigenenergies of both modes strongly depend on the thickness of the metal and both adjacent dielectric layers. We show that both resonances cannot have the same wavelength indicating a clear anticrossing behavior. The experimentally observed splitting of the cavity mode into two resonances is confirmed via transfer matrix calculations.

DOI: 10.1103/PhysRevB.83.033405 PACS number(s): 73.20.Mf, 78.30.Jw, 78.55.Kz, 42.55.Sa

Homogeneous or patterned metal layers are ubiquitous elements of optoelectronic devices such as sensors, solar cells, or light emitting diodes. Besides, metal electrodes also play a crucial part in the realization of an electrically pumped microcavity laser[1–3] and of future devices like electrically pumped polariton lasers.[4–6] The complex interplay between a metal layer and a periodic dielectric structure—such as a distributed Bragg reflector (DBR)—results in the formation of localized surface states at their interface. These so-called optical Tamm states were recently predicted[7–9] and experimentally demonstrated[10,11] with interesting features: Localized inside the DBR stop band with a parabola-like dispersion $\omega(\vec{k}_{xy})$, Tamm states exhibit an in-plane wave vector close to zero and can therefore be excited via photons. Their eigenenergy depends on the thicknesses of both the metal layer itself and of the adjacent dielectric layer.

Recently, a more complex geometry was studied theoretically by Kaliteevski *et al.*[12] The authors demonstrated that a metal layer on top of a microcavity with an embedded quantum well generates hybrid optical Tamm states, which consist of polaritons coupled to Tamm surface plasmons. Further, Bellessa *et al.*[13] observed the strong coupling between such excitons and surface plasmons in an organic semiconductor coated with a metal film. The resulting coherent mixed state is an exciton-plasmon polariton. Tamm states have been utilized by Liew *et al.*[14] to realize exciton-polariton integrated circuits. They discussed the electrical sensitivity of Tamm-plasmon-exciton-polariton modes to generate and control bistable states in semiconductor microcavities.

In this Brief Report, we study the impact of a thin metal layer incorporated into a dielectric microcavity. The optical properties of the device are obtained experimentally and confirmed via transfer matrix calculations. By varying the metal thickness (see Fig. 1), we demonstrate that this layer configuration can be used to shift and split the cavity mode, which is in agreement with the previously mentioned theoretical works. Remarkably, the additional absorption of the metal layer does not suppress the intensity of the hybrid modes but instead enhances them.

The sample studied is made of two DBRs with an active layer in between, which, in our case, consists of the host-guest system of tris-8-hydroxyquinoline aluminum (Alq_3) doped with 2 wt% of 4-dicyanomethylene- 2-methyl-6-p-dimethylaminostyryl-4H-pyran (DCM). The organic host material exhibits a wide absorption band centered around 400 nm and the guest material a 100 nm-wide emission band with a maximum close to 630 nm. The optical thicknesses of the half-wavelength organic cavity layer and the 21 TiO_2/SiO_2 quarter-wavelength layers of the DBR are adjusted to match the cavity resonance (λ_c) and the center of the DBR stop band at 630 nm. The silver is evaporated onto the first DBR through a shadow mask, creating areas with different semitransparent silver thicknesses from 0 to ∼40 nm. After evaporating the Alq_3 : DCM cavity layer and subsequent fabrication of the upper DBR, three types of hybrid cavities result: First, a planar $\lambda_c/2$-microcavity (left in Fig. 1), which features a high quality factor (Q factor) and a very low lasing threshold under optical excitation.[15] Second, a metal-organic microcavity with a wedge-shaped silver layer exhibiting a monotonous thickness gradient of around $0.4\,\frac{\text{nm}}{\mu\text{m}}$ up to a thickness of ∼40 nm (center in Fig. 1), and third, a microcavity with a homogeneous metal thickness of ∼40 nm (right in Fig. 1).

The sample is investigated at room temperature in the transmission geometry of a μ-photoluminescence microscope setup. The beam of a 405 nm cw diode laser is focused by a microscope objective (×25, NA 0.5) through the bottom DBR into a spot diameter $\leqslant 2$ μm to excite one of the three discussed areas. The utilization of such a small spot is important to avoid collecting an emission from areas with different metal thicknesses. The emission is collected by a microscope objective (×63, NA 0.8). A pinhole installed at a distance of 20 cm ensures only to measure the luminescence emitted perpendicular to the sample surface at $k \approx 0$. A 0.6 m spectrograph with a cooled charge-coupled device camera is used to spectrally resolve the output signal.

The measured emission properties of the metal-organic hybrid cavity at normal detection angle ($0^\circ \pm 1.5^\circ$) are depicted in Fig. 2(a). A sharp cavity mode at 632 nm is visible

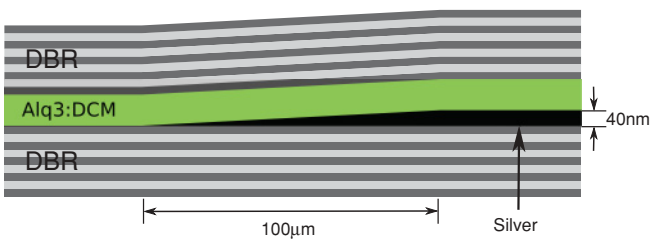

FIG. 1. (Color online) Schematic cross section of the organic microcavity with an embedded metal layer. The wedge-shaped silver layer exhibits a thickness of 0 to 40 nm across a distance of 100 μm.

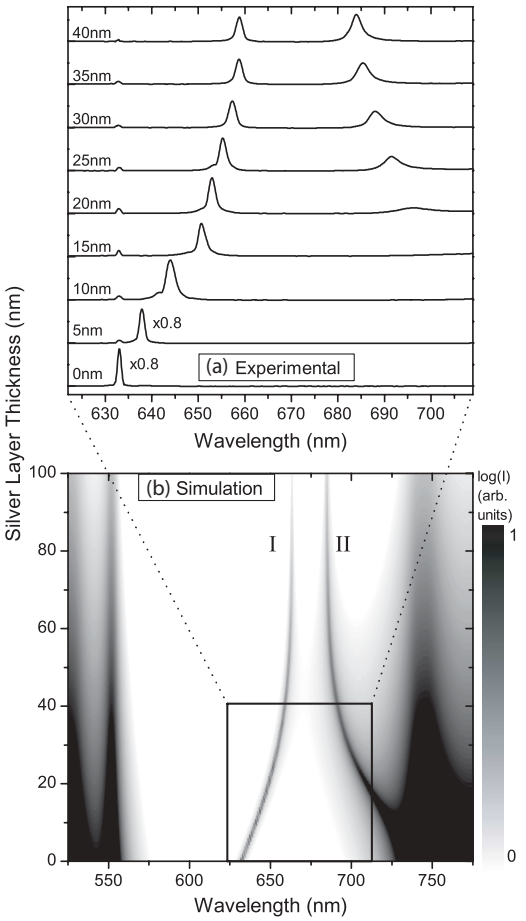

FIG. 2. (a) Emission spectra of the microcavity recorded at different silver thicknesses from 0 to 40 nm (approx. values). Both peaks approach each other down to a minimal separation. The intensity of the original cavity resonance decreases drastically. (b) Numerically simulated transmission spectra for a microcavity with an incorporated silver layer of continuously variable thickness.

when no metal is present inside the cavity. The corresponding Q factor at this position is approximately 800. When the excitation spot approaches and crosses the metal border, a new line emerges in addition to the cavity mode and shifts to larger wavelengths with increasing metal thickness. The Q factor obtained from this resonance (I) is still on the order of 400. For silver layers thicker than ∼20 nm a second new line evolves from the long-wavelength sideband of the DBRs, moving to higher energies with increasing silver thickness. At the same time, the emission into the cavity resonance decreases substantially while the intensities of the two new lines increase. Both new features converge until reaching a certain constant separation (of ∼26 nm) at silver thicknesses above 35–40 nm.

Our sample includes a thin silver layer on top of a periodic DBR with an adjacent high-refractive index quarter-wavelength layer. Therefore, we expect the formation of a superimposed metal-cavity state, similar to the Tamm plasmon-polariton states at the interface of metal and DBR.[8] Additionally, the sample features a second DBR and a half-wavelength organic cavity layer on top of the silver layer (see Fig. 1). This metal-dielectric microcavity exhibits a strong localization of the electromagnetic field near the interface between cavity and metal.[16] According to the considerations in Ref. 12—describing the case of a cavity with a metal layer on top of the DBR—we expect the coexistence of two hybrid cavity-metal resonances in our structure.

To verify this interpretation, we use a transfer-matrix formalism[8,17] to numerically determine the transmission properties of a half-wavelength organic microcavity with different silver thicknesses [Fig. 2(b)]. At zero silver thickness, only one cavity resonance (I) exists at the design wavelength $\lambda_c = 632$ nm. Upon increasing the silver thickness up to ∼40 nm, we observe a continuous shift of the cavity resonance towards lower energies and the emergence of a new mode (II) from the DBR side band shifting to higher energies. Both spectral movements of the modes saturate at a silver thickness of ∼40–50 nm, at a minimal spectral distance of 22 nm. Any further increase of the metal thickness merely leads to a decrease of the overall electric field amplitudes due to a higher absorption in the silver.

The eigenenergies of both modes do not only depend on the thickness of the metal layer and the adjacent high-refractive index layer of the DBR,[8] but also on the thickness of the cavity layer, as shown in Fig. 3. Here, we plot the numerically calculated transmission spectra of our microcavity, incorporating a 40 nm silver layer and varying the thickness of the cavity layer itself. It is visible that, at cavity layer thicknesses of $\lambda_c/4$ and $3\lambda_c/4$, only one state (II) is located in the stop band. At any other thickness of the cavity layer, two states simultaneously exist: Resonance I shows a significant red shift across the stop band as the cavity thickness increases.

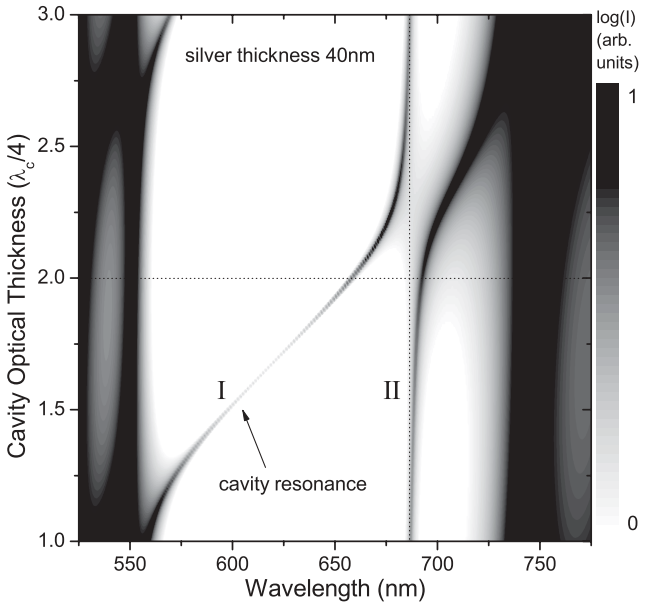

FIG. 3. The simulation shows the dependence of the eigenenergies of the Tamm states on the thickness of the dielectric cavity layer. Both resonances cannot occupy the same wavelength in the stop band, which is identified with an anticrossing behavior (dotted vertical line). The dotted horizontal line indicates the position where experimental data are recorded.

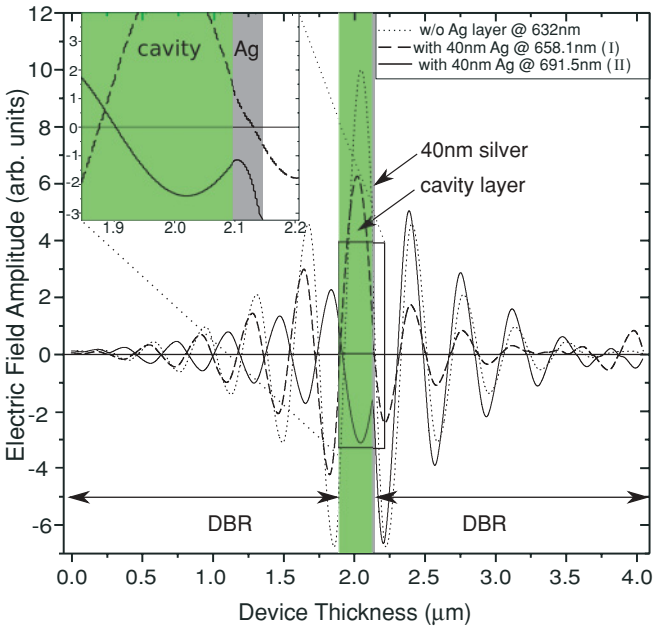

FIG. 4. (Color online) Snapshot in time of the electric field distribution inside the stack for three cases. The incident electric field has unit amplitude, coming from the right. The dotted curve depicts the field at the design wavelength of 632 nm of a microcavity without any metal, as a reference. The dashed and the solid lines are the fields for both resonant modes with an embedded silver layer of 40 nm thickness. After crossing the metal layer, both modes have nearly opposite phases.

However, resonance II depends only weakly on the cavity thickness. At cavity thicknesses of $\lambda_c/2$, anticrossing occurs, demonstrating that two different fields of the same wavelength (i.e., ~686 nm) are not allowed to propagate through such a structure. The underlying origin of this behavior becomes apparent when discussing the electric field distribution inside the metal-organic microcavity for both resonances.

Figure 4 depicts the electric field distribution for both modes (dashed and solid line) inside the hybrid metal (40 nm)-organic microcavity and a cavity without any metal (dotted line). Note that the electric field is incident from the right with unit amplitude. The fields are in phase until they approach the metal layer. For both resonance wavelengths, the amplitudes exhibit a maximum either to the left or to the right of the metal layer. Inside the metal layer, the resonant fields show either minimal intensity or change sign (see inset of Fig. 4). At this point, both modes have nearly opposite phases and therefore would cancel each other at the "crossing" wavelength. This is in agreement with the experimentally observed anticrossing behavior in Fig. 2(a). Strikingly, the electric field amplitude inside the metal layer is not evanescent (solid line), as expected for a metal layer in the absence of a microcavity. Instead, it exhibits a minimum and a subsequent increase, thus reducing the absorption at the resonance wavelength. This explains the rather high peak intensity and the comparatively high Q factors for these hybridized optical Tamm states. Hence, under intense optical pumping these tunable optical Tamm states might lase since the DCM molecules cover a broad gain spectrum.[18] The splitting of the single cavity mode into two coupled optical Tamm states is similar to the fundamental splitting and anticrossing behavior of the bonding and antibonding states in coupled double or multiple quantum wells. The broad emission band supplied by the DCM molecules enables those states to be used for the creation of two monochromatic emissions at different frequencies ω_1 and ω_2 and the observation of spatial and temporal oscillations[19] at the difference frequency ω_1-ω_2. Moreover, tunable optical Tamm states reveal interesting future applications. Research on light-emitting diodes (LEDs) or organic light-emitting diodes (OLEDs) might benefit from this work since the combination of a metal layer and a periodic dielectric structure enables the possibility of properly contacting an active region and exploiting an effective tunable outcoupling through optical Tamm states. In this way it is possible to incorporate an additional thin metal layer to apply fields or inject charge carriers to the cavity region and to gain a further controlling parameter.

In summary, we experimentally observe the transition from a single cavity mode into two optical Tamm states. Despite having only one cavity layer, we observe two coupled resonances whose eigenenergies can be controlled by varying the thickness of the metal layer and the adjacent dielectric layers, respectively. For silver thicknesses of more than 20 nm, both modes are visible. With increasing silver thickness they approach each other but do not cross. The broad emission band of the laser dye DCM allows us to simultaneously investigate the emission properties of both shifting modes. Thus, we demonstrate that the inclusion of a metal layer alters the resonances of a microcavity. However, also the resonator changes the propagation of the resonant mode through the metal layer (i.e., we observe an enhancement of the field inside the metal). We apply a theoretical model based on the transfer matrix method to describe the experimentally observed splitting and shifting of the modes. Thus the existence of hybridized optical Tamm states is not restricted to be solely observable in organic microcavities, but also in inorganic dielectric structures. With respect to constructing optoelectronic devices based on microcavities, such effects must be taken into account.

The authors gratefully acknowledge financial support by the Deutsche Forschungsgemeinschaft (DFG Project No. LE 747/37-1 and LE 747/41-1).

*robert.brueckner@iapp.de

[1] S. Reitzenstein, A. Bazhenov, A. Gorbunov, C. Hofmann, S. Munch, A. Löffler, M. Kamp, J. P. Reithmaier, V. D. Kulakovskii, and A. Forchel, Appl. Phys. Lett. **89**, 051107 (2006).

[2] C. Böckler, S. Reitzenstein, C. Kistner, R. Debusmann, A. Löffler, T. Kida, S. Höfling, A. Forchel, L. Grenouillet, J. Claudon, and J. M. Gerard, Appl. Phys. Lett. **92**, 091107 (2008).

[3]S. Reitzenstein, T. Heindel, C. Kistner, A. Rahimi-Iman, C. Schneider, S. Höfling, and A. Forchel, Appl. Phys. Lett. **93**, 061104 (2008).
[4]D. Bajoni, E. Semenova, A. Lemaître, S. Bouchoule, E. Wertz, P. Senellart, and J. Bloch, Phys. Rev. B **77**, 113303 (2008).
[5]A. A. Khalifa, A. P. D. Love, D. N. Krizhanovskii, M. S. Skolnick, and J. S. Roberts, Appl. Phys. Lett. **92**, 061107 (2008).
[6]S. I. Tsintzos, N. Pelekanos, G. Konstantinidis, Z. Hatzopoulos, and P. G. Savvidis, Nature (London) **453**, 372 (2008).
[7]I. A. Shelykh, M. Kaliteevskii, A. V. Kavokin, S. Brand, R. A. Abram, J. M. Chamberlain, and G. Malpuech, Phys. Stat. Sol. **204**, 522 (2007).
[8]M. Kaliteevski, I. Iorsh, S. Brand, R. A. Abram, J. M. Chamberlain, A. V. Kavokin, and I. A. Shelykh, Phys. Rev. B **76**, 165415 (2007).
[9]S. Brand, M. A. Kaliteevski, and R. A. Abram, Phys. Rev. B **79**, 085416 (2009).
[10]M. E. Sasin, R. P. Seisyan, M. A. Kalitteevski, S. Brand, R. A. Abram, J. M. Chamberlain, A. Y. Egorov, A. P. Vasil'ev, V. S. Mikhrin, and A. V. Kavokin, Appl. Phys. Lett. **92**, 251112 (2008).
[11]C. Symonds, A. Lemaître, E. Homeyer, J. C. Plenet, and J. Bellessa, Appl. Phys. Lett. **95**, 151114 (2009).
[12]M. Kaliteevski, S. Brand, R. A. Abram, I. Iorsh, A. V. Kavokin, and I. A. Shelykh, Appl. Phys. Lett. **95**, 251108 (2009).
[13]J. Bellessa, C. Bonnand, J. C. Plenet, and J. Mugnier, Phys. Rev. Lett. **93**, 036404 (2004).
[14]T. C. H. Liew, A. V. Kavokin, T. Ostatnicky, M. Kaliteevski, I. A. Shelykh, and R. A. Abram, Phys. Rev. B **82**, 033302 (2010).
[15]M. Koschorreck, R. Gehlhaar, V. G. Lyssenko, M. Swoboda, M. Hoffmann, and K. Leo, Appl. Phys. Lett. **87**, 181108 (2005).
[16]D. G. Lidzey, D. D. C. Bradley, M. S. Skolnick, T. Virgili, S. Walker, and D. M. Whittaker, Nature (London) **395**, 53 (1998).
[17]A. V. Kavokin, I. A. Shelykh, and G. Malpuech, Phys. Rev. B **72**, 233102 (2005).
[18]B. Schütte, H. Gothe, S. I. Hintschich, M. Sudzius, H. Fröb, V. G. Lyssenko, and K. Leo, Appl. Phys. Lett. **92**, 163309 (2008).
[19]V. Agarwal, J. A. del Río, G. Malpuech, M. Zamfirescu, A. Kavokin, D. Coquillat, D. Scalbert, M. Vladimirova, and B. Gil, Phys. Rev. Lett. **92**, 097401 (2004).